

9.0%

Date: 2022-10-31 10:14 UTC

\* All sources 32 | Internet sources 32

- [0] [www.frontiersin.org/articles/870299](http://www.frontiersin.org/articles/870299)  
4.7% 106 matches

---

- [1] [www.frontiersin.org/articles/10.3389/feart.2022.849079/full](http://www.frontiersin.org/articles/10.3389/feart.2022.849079/full)  
3.0% 95 matches

---

- [2] [www.hindawi.com/journals/mpe/2018/6843923/](http://www.hindawi.com/journals/mpe/2018/6843923/)  
1.0% 41 matches

---

- [3] [link.springer.com/article/10.1007/s10712-021-09638-4](http://link.springer.com/article/10.1007/s10712-021-09638-4)  
1.2% 35 matches

---

- [4] [www.tandfonline.com/doi/full/10.1080/17415977.2019.1567725](http://www.tandfonline.com/doi/full/10.1080/17415977.2019.1567725)  
0.4% 27 matches

---

- [5] [ur.booksc.me/book/67458809/3ad2a3](http://ur.booksc.me/book/67458809/3ad2a3)  
0.2% 16 matches

---

- [6] [www.tandfonline.com/doi/full/10.1080/27658511.2022.2125905](http://www.tandfonline.com/doi/full/10.1080/27658511.2022.2125905)  
0.0% 13 matches

---

- [7] [www.frontiersin.org/articles/10.3389/fpsyg.2021.509575/full](http://www.frontiersin.org/articles/10.3389/fpsyg.2021.509575/full)  
0.0% 12 matches

---

- [8] [www.sciencedirect.com/topics/earth-and-planetary-sciences/seismic-method](http://www.sciencedirect.com/topics/earth-and-planetary-sciences/seismic-method)  
0.0% 9 matches

---

- [9] [www.researchgate.net/publication/220314009\\_Hybrid\\_intelligent\\_algorithms\\_and\\_applications](http://www.researchgate.net/publication/220314009_Hybrid_intelligent_algorithms_and_applications)  
0.0% 8 matches

---

- [10] [www.frontiersin.org/articles/10.3389/feart.2021.648342/full](http://www.frontiersin.org/articles/10.3389/feart.2021.648342/full)  
0.0% 7 matches

---

- [11] [www.sciencedirect.com/science/article/abs/pii/S0021951716000889](http://www.sciencedirect.com/science/article/abs/pii/S0021951716000889)  
0.0% 5 matches

---

- [12] [www.sciencedirect.com/download.asp?ID=1704287](http://www.sciencedirect.com/download.asp?ID=1704287)  
0.0% 5 matches

---

- [13] [ui.adsabs.harvard.edu/abs/2017AcGeo..65..627K/abstract](http://ui.adsabs.harvard.edu/abs/2017AcGeo..65..627K/abstract)  
0.0% 6 matches

---

- [14] [archive.org/download/frameworkforinco00bono/frameworkforinco00bono\\_djvu.txt](http://archive.org/download/frameworkforinco00bono/frameworkforinco00bono_djvu.txt)  
0.0% 4 matches

---

- [15] [www.researchgate.net/publication/345354335\\_Metaheuristic\\_optimization\\_algorithms\\_to\\_estimate\\_statistical\\_distribution\\_parameters\\_for\\_characterizing](http://www.researchgate.net/publication/345354335_Metaheuristic_optimization_algorithms_to_estimate_statistical_distribution_parameters_for_characterizing)  
0.3% 1 matches

---

- [16] [www.mdpi.com/2077-1312/7/9/326/htm](http://www.mdpi.com/2077-1312/7/9/326/htm)  
0.0% 4 matches

---

- [17] [www.sciencedirect.com/topics/physics-and-astronomy/remanent-magnetization](http://www.sciencedirect.com/topics/physics-and-astronomy/remanent-magnetization)  
0.0% 2 matches

---

- [18] [www.researchgate.net/publication/359414239\\_A\\_Novel\\_Method\\_for\\_Estimating\\_Model\\_Parameters\\_From\\_Geophysical\\_Anomalies\\_of\\_Structural\\_Faults](http://www.researchgate.net/publication/359414239_A_Novel_Method_for_Estimating_Model_Parameters_From_Geophysical_Anomalies_of_Structural_Faults)  
0.0% 2 matches

---

- [19] [www.sciencedirect.com/science/article/abs/pii/S0020025519304220](http://www.sciencedirect.com/science/article/abs/pii/S0020025519304220)  
0.0% 2 matches

---

- [20] [www.researchgate.net/figure/A-graphical-representation-of-the-CMA-with-the-horizontal-axis-representing-the-valence\\_fig1\\_236076387](http://www.researchgate.net/figure/A-graphical-representation-of-the-CMA-with-the-horizontal-axis-representing-the-valence_fig1_236076387)  
0.2% 1 matches

---

- [21] [www.researchgate.net/figure/A-Independent-variable-trajectory-horizontal-axis-representing-the-log-value-of-the\\_fig5\\_356509302](http://www.researchgate.net/figure/A-Independent-variable-trajectory-horizontal-axis-representing-the-log-value-of-the_fig5_356509302)  
0.0% 1 matches

---

- [22] [arxiv.org/pdf/2009.09471](http://arxiv.org/pdf/2009.09471)  
0.0% 3 matches

---

- [23] [www.researchgate.net/figure/Test-time-evaluated-using-different-methods\\_fig7\\_324987100](http://www.researchgate.net/figure/Test-time-evaluated-using-different-methods_fig7_324987100)  
0.0% 2 matches

---


- [24] [www.researchgate.net/figure/Sugar-Beet-Seed-Germination-Trial-Another-notable-observation-was-that-the-wet-heat\\_fig5\\_307090539](http://www.researchgate.net/figure/Sugar-Beet-Seed-Germination-Trial-Another-notable-observation-was-that-the-wet-heat_fig5_307090539)  
0.0% 2 matches

---


- [25] [link.springer.com/article/10.1007/BF00878921](http://link.springer.com/article/10.1007/BF00878921)

0.0% 1 matches

---

[26]  www.sciencedirect.com/science/article/pii/S2288430017301823  
0.0% 1 matches


---

[27]  www.sciencedirect.com/science/article/abs/pii/S092698511100070X  
0.0% 1 matches


---

[28]  ur.booksc.me/book/7152617/faa07b  
0.0% 1 matches


---

[29]  pubmed.ncbi.nlm.nih.gov/27610303/  
0.0% 1 matches

---

[30]  ur.booksc.me/book/343661/b51a9c  
0.0% 1 matches

---

[31]  pubmed.ncbi.nlm.nih.gov/35251303/  
0.0% 1 matches

---

25 pages, 5934 words

**PlagLevel: 9.0% selected / 19.6% overall**

186 matches from 32 sources, of which 32 are online sources.

#### Settings

Data policy: *Compare with web sources*

Sensitivity: *High*

Bibliography: *Bibliography excluded*

Citation detection: *Highlighting only*

Whitelist: --

<sup>[1]</sup> Investigating the applicability of the Social Spider Optimization for the inversion of magnetic anomaly caused by dykes

## Abstract

The geologic relevance of dipping dykes is enormous. They are very crucial structures for hydrogeologic, geothermal, and hydrocarbon investigations.<sup>[1]</sup> However, due to its characteristic complexity, no specific technique has been generally accepted for the interpretation of dykes from magnetic data. This study designs and trial-tests a new method based on the social spider optimization (SSO) algorithm. The design process targeted at deciphering the physical properties defining amplitude, depth of burial, half-width, and inclination of the anomaly was presented in a detailed and straightforward manner. The test data consisted of synthetically generated anomalies corrupted with random noise at different levels, and field anomalies extracted from mining records from China and Turkey. The new technique's capability and effectiveness in resolving each of the inverse problems were outstanding. Deductions from results imply the SSO as a robust tool, stable and efficient for deciphering the physical characteristics of deep and shallow-seated dykes from magnetic data.<sup>[0]</sup> Therefore, it is recommended for the inversion of other geophysical data such as self-potential and gravity data.

Keywords: Anomaly; Dyke; Inversion; Spider; Magnetics; Interpretation

## 1 Introduction

Modeling in geology generally involves gathering and assembling geological information such as core cutting, sections, panels, and maps to generate models that, in tradition, should be replicas of the subsurface. While the final products of this technique have been very

accurate and reliable, the process of acquiring this information, particularly in areas of little or no exploration history, is usually laborious costly, and time-consuming. To this end, the geophysical approach is widely preferred. Geophysical data used in imaging geologic structures buried at various depths below the Earth's surface are usually acquired using any of the conventional geophysical methods (Ben et al, 2022c). The geophysical exploration methods are many and each exploits variations in physical properties with respect to the conventional local or regional normal.

Amongst all the conventional geophysical techniques, the magnetic method is the oldest, and reliable. Over the years, it has found success in the search for hidden ores and structures associated with mineral deposits. Field readings, representing spatial variations in magnetic field strengths are always corrected at first – and in the best possible ways, to free the raw data of contributions from extraneous sources.<sup>[1]</sup> With the advent and application of high-speed computers, artificial intelligence, tools developed have greatly improved the quality of data collection and general confidence in existing processing techniques (Ben et al., 2021c; Mbonu and Ben, 2021; Mbonu et al., 2021). However, the situation with interpretation is not similar, as the deciphering of geologically relevant information of magnetic data still relies heavily on subjectivity and geologic history. Conventionally, magnetic anomaly data are interpreted in terms of the depths of burial, geometry, and susceptibility of the causative structure. Inversion procedures are commonly adopted for the unraveling of these causative structures.

Inverse modeling in geophysics aims at unravelling characteristic parameters of a structural features through procedural matching with existing and/or numerically constructed models (Essa and Elhussein, 2020). The structures of interest in mineral exploration usually

include ores, faults, dykes and contacts; and all modelling procedures seek at determining the parameters that can unravel the in situ position, depth, and shape of these interests.

The geologic relevance of dipping dykes is enormous. Triassic dykes have been known to impound fracture induced groundwater; dipping dykes are also practical heat contacts in most geothermal systems as well as effective traps for hydrocarbons. More too, dipping have proven to influence local/regional direction of mineralization (Li et al., 2019; FitzGerald, 2018). However, no technique has been exclusively accepted for the inversion of this geologic structure.

Over the years, several techniques have been adopted for the interpretation of dyke-related anomalies. Some of these procedures exploit computational formulations including the gradient method (Radhakrishna-Murthy et al., 1980), iteration method, fair function minimization (Tlas and Asfahani, 2011; Abdelrahman et al., 2012). Others have experimented with procedures consistent with the Gauss method (Won,1980), least squares (Abo-Ezz and Essa, 2016), wavelet transform (Gholghasi et al.,<sup>[1]</sup> 2009), and **simplex algorithm** (Tlas and Asfahani, 2015).<sup>[0]</sup> Nonetheless, results show that these numerical approaches are frequently characterized by a large number of **invalid solutions**, which have been attributed to noise sensitivity, improper filtering, **window size compatibility** and, most importantly, an overreliance on geologic history that **may not be reliable or available**. With increased improvements in machine learning and artificial intelligence (Ewees et al., 2019), practitioners have shown that these problems can be attenuated with the instrumentality of evolutionary techniques. Al-Garni (2015) used modular neural network inversion to estimate parameters of dipping dikes. Balkaya and Kaftan (2021) employed a differential search technique to interpret magnetic anomalies induced by 2D dyke-shaped

structures.<sup>[1]▶</sup> Essa and Elhussein (2020) presented a strategy based on the robust Particle Swarm Optimization and employed the same for the investigation for magnetic data by a 2D dipping dyke. Di Maio et al (2020) modeled magnetic anomalies generated by common geological structures including dykes with the Genetic-Price inversion algorithm. Biswas and Acharya (2016) interpreted and modeled a vertically magnetized semi-infinite vertical rod-type structure using the very fast simulated annealing (VFSA) global optimization approach.<sup>[1]▶</sup> Ekinci (2016) developed a Matlab-based algorithm for the estimation of depth isolated thin dykes by using higher-ordered horizontal derivatives calculated from magnetic anomalies. Ekinci et al. (2017) achieved analytic signal amplitude inversion of magnetic anomalies over thin dykes using differential evolution. Balkaya et al. (2017) conducted three dimensional magnetic inversion of intrusives using the differential evolution metaheuristic technique. Balkaya et al. (2015) inverted magnetic anomalies due to two dimensional dykes using the differential evolution algorithm. Ben et al. (2021b) designed an innovative system for the understanding of dyke systems using the Manta Ray Foraging Optimization procedure.<sup>[3]▶</sup> Srivastava and Agarwal (2010) inverted the amplitude of the 2-D analytic signal of magnetic anomaly over dykes using the particle swarm optimization technique. Vashisth et al. (2020) presented a Whale optimization approach for the inversion of anomalies due to vertical and dipping dykes. These intelligent algorithms, which mainly imitate normal behaviors in nature, have proven superior and efficient in overcoming most challenges posed by the classical methods. The strength of these algorithms is drawn from the fact that, unlike other algorithms, the search for feasible solutions is independent of gradient. As is well known, gradients are usually more difficult to resolve with increase in complexity such as that characterize dipping structural features.<sup>[1]▶</sup>

In this paper, we present a new stochastic technique for interpreting magnetic anomalies over dipping dyke geologic features. The new strategy is based on the recently proposed SSO algorithm.

The SSO is a bio-inspired metaheuristic that imitates the mutual behaviors of social spiders (Tamilarasi et al., 2021; Cuevas, Zaldívar, et al., 2018). Unlike other heuristic algorithms where optimization follows swarms of one agent type in a search domain, the SSO concurrently exploits the operational behavior of both male and female spiders (the agents) searching for space. A set of gender-dependent operations is used to guide the positions of the agents towards an optimal solution satisfying the objective. So because the algorithm promotes individually categorized traits over swarm traits, the collective behavioral results of this personalized characterization are healthy cutbacks in critical particle concentration defects, which are common in most metaheuristic procedures such as GA, DE, and PSO (Cai and Cui, 2010; Nguyen et al., 2020; Sun et al., 2019). The SSO has been successfully employed in diverse fields including engineering (Fathy et al., 2020), agriculture (Thilagavathi and Amudha, 2019), pharmacy (Sahlol et al., 2019), energy (Tabasi and Asgharian, 2019) amongst many others. Reports from these applications, increasingly promise the SSO algorithm as a meaningful and appropriate inversion tool for geophysical data inversion.<sup>[0]</sup> However, at the time of preparing the initial draft of this article, no application of SSO in dyke inversion has been reported in literature.

## 2. Methodology

<sup>[20]</sup>▶  
2.1 Forward modeling of a 2-D dipping dyke

(1) expresses the magnetic anomaly ( $y_i, K, h, z, \alpha$ ) of the structure at any point  $y_i$  on the sampling profile, assuming a Cartesian coordinate system with the vertical axis representing the strike of the buried dipping dyke buried at depth  $z$  from the surface and the horizontal axis representing the sampling profile.

$$F(y_i, K, h, z, \alpha) = K \left[ \sin \alpha \left( \tan^{-1} \left( \frac{y_i+h}{z} \right) - \tan^{-1} \left( \frac{y_i-h}{z} \right) \right) - \frac{\cos \alpha}{2} \ln \left( \frac{(y_i+h)^2 + z^2}{(y_i-h)^2 + z^2} \right) \right] \quad (i = 1, 2, \dots, N),$$

(1)

where  $\alpha$  is the index angle,  $h$  - the half-width,  $z$  is the depth, while  $K$  represents amplitude of the anomalous structure. Table 1 shows the amplitude coefficients and index angles for total, horizontal, and vertical fields, where  $j$  is the geomagnetic inclination (represented by the angle between the profile direction and the geomagnetic field direction),  $\lambda$  is the profile azimuth with respect to magnetic north (Figure 1),  $m$  is the susceptibility contrast and  $\delta$  is the dipping angle, and  $m$  is the susceptibility contrast.

The process around deciphering the set of parameters that describe the buried structure from the magnetic data. The search for the inverse problem solution is as described by Ben et al., 2021b, and, Ben et. al., 2022b. This initial model is normally constructed with knowledge from historical information such as drilling logs, and data from other geophysical surveys.<sup>[1]</sup>▶ The model is progressively improved through series of optimization



processes based on the cost function (2) until the fitted version estimating data synonymous or very near-synonymous with the observed data is obtained

$$\text{objective function} = \frac{\sum_{i=1}^n (F(\mathbf{y})_i^m - F(\mathbf{y})_i^e)^2}{n}$$

where  $F(\mathbf{y})_i^m$  and  $F(\mathbf{y})_i^e$  are respectively the magnetic anomaly from observed data and those estimated using the proposed methodology while  $n$  is the data number

## 2.2 Social spider optimization

The SSO is a heuristic procedure introduced by Cuevas et al. (2013). The algorithm operates by mimicking the cooperative behaviour of social spiders where both the female and male spiders work together as search agents. <sup>[15]</sup> The spiders move randomly within the search space in a high-dimensional communal spider web where each spider is promoted as a candidate solution (Alrashidi et al., 2020). The algorithm, designed to use their behavioural pattern in solving the magnetic inversion problem, was implemented in seven stages as follows:

Stage 1: First, the male and female population vectors of spiders (representing magnetic models or search agents) were randomly initiated in search space. Each member of this population was taken as a prospective solution to our geophysical problem. Considering that the density of female spiders is usually more than the density of male spiders (0.65-0.90) of a conventional colony population,  $S$ , the number of female spiders,  $N_f$  was generated using (7) (Yu and Li, 2015; Alrashidi et al., 2020) as;

$$N_f = \text{Floor} [0.9 - \text{rand} \times 0.25]. S ,$$

(7)

where, rand is a random number in the range [0,1]. Resultantly, the male population  $N_m$  was calculated using (8);

$$N_m = S - N_f,$$

(8)

We also assumed that  $S$ , a union of females  $f$  and  $m$  contains  $N$  elements such that  $S = \{s_1 = f_1, s_2 = f_2, \dots, s_{N_f} = f_{N_f}, s_{N_f+1} = m_2, \dots, s_N = m_{N_m}\}$ .

Stage 2: At this stage, some weight,  $G$  was assigned to all the spiders. The weight was used to rate the quality/superiority of spiders in  $S$ .  $G_i$  was determined from (9) as

$$G_i = \frac{Z(s_i - S_w)}{S_b - S_w},$$

(9)

where,  $Z$  is the fitness value of a spider evaluated using the objective function while  $S_w$  and  $S_b$  respectively correspond to the worst and best individuals in the search space.  $S_b$  and  $S_w$  were defined as expressed in (10) and (11) (Fathy et al., 2020; Ben et al., 2022a);

$$S_b = \max_{i \in (1,2,3,4,\dots)} (Z(S_i)),$$

(10)

$$S_w = \min_{i \in (1,2,3,4,\dots)} (Z(S_i)),$$

(11)

Stage 3: Next, the agent's vibration process (VB) was simulated. Vibrations of social spiders are synonymous with their movement. This stage was numerically implemented using (12);

$$VB_{i,j} = Z_j \times \exp(-X_{i,j}^2),$$

(12)

where,  $X_{i,j}$  is the Euclidian distance between spiders  $i$  and  $j$ .

Stage 4: After establishing their vibration structure, we initialized the position of the agents in the search space. As earlier explained, this represents the initial model for our dyke problem. As such, this initial position vector for each spider,  $f_i$  or  $m_i$ , is constructed as a 4-D vector populated by the parameters to be optimized ( $K$ ,  $h$ ,  $\alpha$ , and  $z$ ). The parameter values were generated within the space-dependent lower,  $LB_j$  and upper,  $UB_j$  bounds ((13) and (14)) (Fathy et al., 2020)

$$f_{i,j}^o = B_j^{low} + rand().(B_j^{high} - B_j^{low}) \quad i = 1,2, \dots, N_f; j = 1,2,3,4,$$

(13)

$$m_{k,j}^o = B_j^{low} + rand().(UB_j - LB_j) \quad k = 1,2,3 \dots, N_m; j = 1,2,3,..$$

(14)

Stage 5: For each iterative session, the co-operative interaction between individual spiders in the colony was implemented according to the spider gender.

That of the female spiders was done using (15) (Husodo et al., 2020).

$$f_i^{(k+1)} = \begin{cases} f_i^{(k)} + \alpha \cdot VB_{i,c} \cdot (s_c - f_i^{(k)}) + \beta \cdot VB_{i,b} \cdot (s_b - f_i^{(k)}) + \delta \cdot (\text{rand}() - \frac{1}{2})V \\ f_i^{(k)} + \alpha \cdot VB_{i,c} \cdot (s_c - f_i^{(k)}) + \beta \cdot VB_{i,b} \cdot (s_b - f_i^{(k)}) + \delta \cdot (\text{rand}() - \frac{1}{2}) \geq V \end{cases}, \quad (15)$$

where,  $\alpha$ ,  $\beta$ ,  $\delta$ , and  $\delta$  are random numbers within the range of 0 and 1,  $k$  is the  $t$  maximum iteration number,  $V$  the probability factor, and  $s_c$  and  $s_b$  are the nearest best to the  $i$ th spider, and the population  $S$  best spider, respectively.

The co-operative behaviour of male spiders was defined using (16). In conventional colonies, male spiders are usually dominant and non-dominant. The dominant males boasting of better fitness values usually have greater chances of attracting female mates, while the non-dominant ones, rather gather in male population centres to exploit resources lost or leftovers from the dominant ones. These behaviours were simulated numerically as; (Shayanfar et al., 2016)

$$m_i^{(k+1)} = \begin{cases} m_i^{(k)} + \alpha \cdot VB_{i,f} \cdot (s_f - m_i^{(k)}) + \delta \cdot (\text{rand} - \frac{1}{2}) & \text{if } W_{N_{f+i}} W_{f+m} \\ m_i^{(k)} + \alpha \cdot \left( \frac{\sum_{h=1}^{Nm} m_h(k) \cdot W_{N_{f+h}}}{\sum_{h=1}^{Nm} W_{N_{f+h}}} m_i(k) \right) & \text{if } W_{N_{f+i}} W_{f+m} \end{cases}$$

(16)

where,  $S_f$  is the nearest female spider to male spider  $i$  and the term  $\left( \frac{\sum_{h=1}^{Nm} m_h(k) \cdot W_{N_{f+h}}}{\sum_{h=1}^{Nm} W_{N_{f+h}}} \right)$  is an average value for the population's male spiders.

Stage 6: In this stage, we carried out the selection of offspring for the next generation. As in most evolutionary algorithms, this is an important part of the model's evolution to the solution. To produce the next generation of spiders, mating between dominant males and females was permitted within a specified radius ( $R$ ) computed using (17) (Klein et al.,

2016). The fitness values of the next generation of dominant spiders were then evaluated and compared to those of their parents. If new spiders outperformed their parents in terms of quality, the young spiders were adopted and their parents replaced.

$$R = \frac{\sum_{j=1}^4 (UB_j - LB_j)}{8} \quad (17)$$

In this study, the ranges of UB and LB for each of the parameters were selected based on subjective deductions from prior petrophysical or geophysical deductions.

At the end of every successive iteration, the quality of results obtained in that particular stage was evaluated by calculating the misfit between the measured and estimated data using (6). It should be added that (6) is basically the root mean square error (RMS). Once a suitable RMS was arrived at, the four physical parameters (K, h,  $\alpha$ , and z) were returned.

Figure 2 is a summarized flowchart highlighting the stages implemented for the SSO procedure.

### 2.3 Remanent magnetization

It should be stated that the measured magnetic field measurements used for this study were construed as exclusive responses to induced magnetization. To this end, signals resulting from remanent magnetization were considered to be so minimal that their impacts could be considered negligible, or their responses had been filtered out. Further, irregularities in the inversion results due to poor field data wrangling or erroneous excision of the regional field are likely to deteriorate inversion results and cannot be wholly used to judge the efficacy of the new technique.

## 2.4 Anomaly origin

The precise location of the anomaly's origin is vital for interpreting dipping dykes. A common approach adopted by some authors is to select a forward model that approximates the dyke structure to a thin sheet model (Cooper, 2015; Ekinici, 2016; Ekinici et. al, 2017) and estimate the origin as one of the model parameters. While this technique gives good estimations, its efficiency decreases with an increase in thickness and the vertical extent of the intrusive (Hinze et al., 2010; Roy, 2008). Another approach is to exploit the fact that for a dykes magnetized due to induction, the profile curve is symmetric about the origin. The Powell approach which adopts this theory is employed for this study. According to Powell (1967), if point pairs on a profile are located at opposite sides of its x-origin, then the product of their x-coordinates will always be equal to a constant. This means that if the profile has two a and b points such that

$$mg_a = mg_b = mg_{max} - \frac{\text{amplitude}}{2}$$

(18)

and another pair, c and d on the origin's antipodal side such that

$$mg_c = mg_d = mg_{max} + \frac{\text{Amplitude}}{2}$$

(19)

then, at an assumed origin at distance  $\tau$  from the true one,

$$(a + \tau) \cdot (c - \tau) = (b + \tau) \cdot (d - \tau)$$

(20)

Rearranging;

$$\tau = \frac{b \cdot d - a \cdot c}{(b - d) - (a - c)}$$

(21)

Correspondingly, at origin = 0,

$$a \cdot c = b \cdot d$$

(22)

## 2.5. Algorithm design/complexity

The program employed for the SSO process was designed in python3. The VSCode IDE used for compiling the program was installed on a simple Windows 10 desktop running with a Core i5 processor.<sup>[1]</sup>

For complexity, the program's duration varied based on the complexity of the structure modeled.<sup>[1]</sup> Howbeit in all cases, the optimization process rounded up in less than 20 seconds.

## 2.6<sup>[0]</sup> Uncertainty analysis

Because of the non-linearity, non-uniqueness, and ill-posedness of geophysical inverse problems, it is a well-known fact that several models built from heterogeneous parameter sets can fit well into similar observed measurements at the same time. This occurrence frequently causes significant uncertainty in parameters estimated for these inverse problems. As a result, uncertainty assessment analyses have come to be recognized as critical in inversion investigations (Connolly and Khan, 2016).

The Bayesian method has been used to estimate model parameters that describe stochastic changes. The approach is founded on the idea of conditional probabilities. Prior probability distributions of the needed parameters could be derived by combining priori information with the likelihood of experimental data (Pallero et al., 2017; Ekinici et al., 2020; Pangilinan et al., 2008).<sup>[0]▶</sup> For global optimization algorithms like SA, PSO, and GA, correct sampling has been achieved with the Markov-Chain Monte Carlo algorithm (Mosegaard & Tarantola, 2002; Yusof et al., 2018). For this investigation, the Metropolis-Hasting algorithm (Metropolis et al., 1953; Hastings, 1970), was employed for parameter sampling. The Metropolis-Hasting (MH) method suggests various models based on some prior distribution.<sup>[0]▶</sup> The likelihood of each proposed model is computed by solving the forward problem and calculating the misfit in the data.<sup>[0]▶</sup> If there is an increase in likelihood, the revised model is accepted. Furthermore, even if the likelihood decreases, the proposed model can still be accepted. However, this will be with a probability determined by the likelihood ratio between the suggested and original models.<sup>[0]▶</sup> The method which is based on simulated annealing without cooling schedule allowed for the assessment of uncertainty by providing parameter confidence intervals (Connolly and Khan, 2016). In this study, 500 iterations were allowed for the MH algorithm.

## 2.7 Parameter tuning studies

Most nature-inspired global optimization algorithms have their control parameters that heavily influence the algorithm's convergence point during inversion. These parameters are critical for any algorithm's overall efficiency (Villa-Acuna and Sun, 2020; Granat, 2003). Their selection, however, is largely determined in essence by the considered



problem (Ekinçi et al., 2020). Considering this, model parameters tunings were carried out before inversion to choose the best control parameters for the algorithm.<sup>[0]▶</sup>

To properly guide the tuning studies, a synthetic magnetic anomaly dataset was theoretically generated using (1) with  $K = 60$  nT. Further,  $h=15$  m,  $z=12$  m,  $\alpha = 55^\circ$ , with a profile length of 300 m (Figure 3). For the experiment, broad search spaces (Table 3) were adopted for the model parameters.<sup>[0]▶</sup> The parameter tuning analyses were primarily concerned with determining the best values for the probability factor –  $V$  – and the population of spiders in the search space –  $S$  and their impact on the final solution.<sup>[0]▶</sup> Thirty independent runs consisting of 500 iterations were allowed for the optimization process.  $S$  was set to 120. This value for  $S$  was obtained by multiplying the number of unknown parameters (4) by the number of independent runs (30)(Balkaya and Kaftan, 2021; Turgut, 2021). The magnetic anomaly problem was then statistically analyzed using the standard deviation, mean, and minimum of RMS values obtained. After 30 runs, the results obtained by utilizing various  $V$  are shown in Table 2. From the table, a  $V$  of 0.7 seems to produce the best statistical results (boldfaced). This suggests that using 0.7 as the probability factor for the magnetic data will make the optimization process more stable and efficient. As a result, 0.7 was chosen as  $V$  for the optimization problem. Another observation is the significant error gap between the value of  $V$  that provided the best results and the value that generated the poorest outcomes.<sup>[0]▶</sup> This massive disparity could undoubtedly have a substantial impact on the solution's accuracy in terms of optimal model parameter resolution. This highlights the vital need for parameter tuning studies in global optimization applications.

### 3 Theoretical examples

To validate the performance of the suggested methodology, the algorithm was exposed to several preliminary controlled tests with synthetic anomaly data. The noise-free version of the test data was evaluated first, and then this was purposefully corrupted with varying levels of noise and re-evaluated.

### 3.1 Noiseless anomaly

The SSO algorithm was applied to model noise-free theoretical anomalies for a dike-like structure constructed with model parameters of  $K = 60$  nT,  $\alpha = 55^\circ$ ,  $h = 15$  m, and  $z = 12$  m. The magnetic field anomaly was designed using (1).

<sup>[0]</sup> The search space was populated with 120 initial models based on the parameter space. For the bounds,  $K$  values were set to be between 0 and 500 nT;  $h$  and  $z$  from 0 to 50 m; and  $\alpha$  between  $-90^\circ$  and  $90^\circ$ . 500 repetitive iterations were allowed for each run (Figures 4-6). SSO was found to have strong optimization abilities. <sup>[1]</sup> The corresponding model parameters obtained at the end of the process were respectively are shown in Table 3.

Comparing these estimations with the actual parameters used in designing the model, it is evident that the new method's estimation abilities are considerably excellent. Further, the MH technique was applied for the assessment of uncertainty in these parameters obtained. To carry out the uncertainty appraisal, steps consistent with those outlined in Section 2.7 were adopted. Careful examination of the histogram reconstructed after the appraisal procedure (Figure 6) reveals that our solutions fall within reasonable confidence intervals.

### 3.2 Noisy anomaly

To model real-world scenarios, the synthetic data, which had been previously modeled in Section 3.1, was contaminated with 5, 10, and 20% random noise. The random numbers used in noise were zero-mean and, of course, normally distributed (as with all Gaussian distributions). The standard deviation (SD) of the synthetically added noise content is shown in Table 4. <sup>[0]►</sup> These varied amounts of noise were added with the goal of evaluating the suggested methodology's efficacy under non-ideal settings such as the presence of noise caused by the host materials or adjoining geologic intercalations. The random noise was created automatically using the MATH library and added individually to the synthetic data. The percentage of corruption was computed using (23).

$$\text{Noise percentage} = \frac{\|m_{g_n} - m_{g_i}\|}{\|m_{g_n}\|}$$

23

where  $m_{g_i}$  and  $m_{g_n}$  are the noiseless and noisy anomalies, respectively.

The SSO-based methodology was used once more to estimate the model parameters. <sup>[1]►</sup> To facilitate this task, (2) was used as the cost function, and the model ranges employed with the noiseless example were readopted. After each repetition, the convergence and misfit were examined.

The SSO algorithm-estimated model parameters and their actual values were found to be remarkably consistent (Table 5, Figures 7-9). Another notable observation is that the K parameter (the anomaly's coefficient of amplitude) appeared to be more sensitive to increasing noise than other parameters. <sup>[0]►</sup> This sensitivity, which is likely to alter interpretation when dealing with exceedingly sophisticated and deep-seated dyke systems,

may be explained by the fact that  $K$  plays a multiplier factor role in (1) and can be easily corrected by narrowing the range of the space-bound.<sup>[0]</sup> Furthermore, the results show that the after-convergence misfit and RMS error increase somewhat with noise. Nonetheless, this does not affect the general inversion process because parameter results continuously appeal even at a noise level of 20%. (Table 5). Furthermore, the RMS obtained (Figures 8-10) was found to be well-matched to the standard deviation of the corruptions (Table 4). Uncertainty histograms were constructed based on sampling done by MH and over model parameters for scenarios of the executed noisy models (Figure 10)(For the sake of brevity and paper space, only plots for 10% noise are shown). The histograms reveal that the SSO sampling process is quite effective, as the actual parameter values estimated by the algorithm all fell within high probability regions. These show the SSO technique as being intrinsically stable and as admirably performing even when dealing with noisy datasets.

#### 4 Field examples

The SSO algorithm was experimentally evaluated using two field examples extracted from distinct mining areas in Turkey and Asia.<sup>[0]</sup> The parameters representing the physical characteristics of the subsurface magnetic anomalies were then analyzed and compared to results from previous investigations published in the literature.

##### 4.1 The Magnetite Iron Deposit, China

In the early 1960s, a regional aeromagnetic study in the Western Province of Gansu, China, identified an alluvial covered area afterwards designated M163. M163 has long been investigated and regarded to be a metasomatic contact of iron deposits (Zhang et al., 2019).

Following a rigorous ground magnetic survey, the regional anomaly was sectioned into eleven distinct containing smaller individual anomalies (Scott, 2006; Ben et al., 2021). The M163-1 magnetic anomaly was investigated in this investigation. A 200-m long magnetic anomaly profile (MN) spanning the M163-1 area was collected from a magnetic intensity contour map at 2-m intervals for this purpose (Figure 11).

As the dipping dyke was suspected as a two-dimensional structure based on a priori geologic information, the SSO algorithm was used to estimate its distinctive parameters using the forward model outlined in (1). However, before beginning the iteration process, the upper bounds for  $K$ ,  $h$ , and  $z$  were set to 0 nT,  $-90^\circ$ , 0 m, and 0 m, respectively, and the lower bounds to 20000 nT,  $90^\circ$ , 50 m, and 50 m, respectively (Table 6). The algorithm was set up to run using 30 individuals. The inversion process took around 65 seconds to complete. There were 500 iterations permitted. The model parameters obtained after algorithm execution are displayed in Table 6. The similarity between the estimated and observed anomalies is discernible (Figure 12).

Table 7 compares model parameters produced by earlier researchers using various methods to those obtained by the SSO algorithm in this work. Petrophysical records (Guo et al., 1998) report the thickness of the alluvial overburden to be between 20 and 25 m. Using PSO, Essa and El-Hussein (2017) calculated that the dyke, which he reported as being inclined at  $57.99^\circ$ , is buried at a depth of 22.55 m. In contrast, Ben et al. (2021) used manta ray foraging optimization to identify the physical properties of the Gansu dike. They calculated the anomaly's  $h$  to be 20.10 m and  $\alpha$  as  $60.98^\circ$ . It can be observed that our results are very consistent with those from these reports.

## 4.2 The Bayburt-Sarıhan dyke

In this example, we employed the SSO for the interpretation of a shallow dyke in the Bayburt-Sarıhan skarn zone of Northeastern Turkey. The Bayburt-Sarıhan skarn zone is an extensive geologic zone dominated by granodiorite, limestone, volcanic sediments and tuffs. The granodiorite unit responsible for the steep topography of the mining area is believed to have been deposited earlier. The unit is bounded to the east and in a north-south direction by a Cretaceous limestone unit which is heavily fractured. To the southwest of the skarn zone - and sandwiched limestone and the granodiorite unit, an intrusion mainly composed of magnetite has been reported. We would be analyzing this intrusion.

Figure 13 shows a profile extract of a vertical component magnetic anomaly map constructed for the region (Keskin et al., 1989) showing a 1200 m profile taken over the region. The profile was sampled at an interval of 200 m. Due to the paucity of geologic information for this structure, the bounds were kept open-ended; however, a bisection algorithm was inserted into the SSO structure to prevent indiscriminate movement of the agents. While this increased the cost (time) of the optimization process, it did not affect the quality of results. The results – after convergence, are shown in Table 8 and Figure 13. The RMS of 3.452nT was also impressive.

Aydın and Gelişli (1996) performed some anisotropic magnetic investigations in the region and showed the structure as an eastward dipping dyke with a slope of about  $110^\circ$ , depth of about  $z=100$  m, and a half-width of about  $h=75$ m. Dondurur and Pamukcu (2003) employed the damped least-squares inversion method on the same anomaly. They reported the depth to the dyke as 97m, the inclination as  $111^\circ$ ,  $h$  as 76 m, and  $z$  as 97 m. It can be

discerned from these results, that the SSO produces estimations similar to those obtained by earlier workers (Table 9).

## <sup>[1]▶</sup> 5. Discussion

The new method based on the SSO algorithm was designed for geophysical inverse problems and subjected to a series of tests to gauge its adaptability and suitability for the interpretation of magnetic anomalies due to dipping dyke models. The new tool was tested with data synthetically generated from an already established forward model and examples extracted from real mining fields. The cases allowed evaluation of the new method's viability, strengths, and reputability.

<sup>[2]▶</sup> In terms of performance, the convergence signatures (Figure 5) for all the cases indicate that the SSO possess strong and extensive search abilities. As can be observed, the agents (parameter vectors) are not caved up in the search space. This is not unrelated to the design structure (Section 2). <sup>[2]▶</sup> Popular metaheuristics such as PSO, GA, and SA employ individuals with the same properties and performing nearly the same behaviours. In these cases, algorithms squander the opportunity to add new and selective operators resulting from considering individuals with different characteristics. As the algorithm advances, such characteristics cause the whole population to cluster around the best particle or to diverge indiscriminately, resulting in traditional concerns such as exploration-exploitation imbalance and premature convergence. The SSO, on the other hand, models each individual based on gender. In this case, the entire population is divided into several search-agent groups, and specialized operators are applied to each one selectively and explicitly.

With this framework, extensive exploitation is achieved (16) in such a way that efficient exploration is still maintained (15) – tackling the aforementioned popular problems at a go.

More also, Figure 4 reveals the fast convergence rate of the new method. In most cases, the algorithm converges in less than 150 iterations; and under 200 iterations for all cases.

<sup>[3]</sup>▶ This speed notably, does not affect the quality of the result in any way as the RMS were consistently impressive even for complex noisy and field examples.

The algorithm was tested for sensitivity and stability by corrupting the synthetic data with random noise (Section 3.2). As expected, the results of the noisy data were found to be marginally worse than those of the noise-free counterpart. Nonetheless, as illustrated in figure 9, the inversion procedure remained undisturbed, producing reliable parameters up to the highest level of noise tested (20%).<sup>[0]</sup>▶ As a result, it may be inferred that the new technique is intrinsically adept when dealing with noisy data.

We further tested the new technique with real field data taken from Chinese and Turkish mining fields. As is generally known, it is not always assured that a novel algorithm's virtuosic performance with numerically generated data (which is normally constructed under ideal conditions) would always replicate with real-world data (subjected to heterogeneous factors). Besides confirming the algorithm's capabilities, the outputs of inversion of these anomalies were also similar to those acquired previously using alternative methods and petrophysical investigation.

The previously developed Monte-Carlo approach was used to check for ambiguity in each of the estimations (Section 2.6). The MH sample algorithm uncertainty analysis positioned the geophysical parameters predicted by the design technique within exceptionally high



probability regions, increasing dependability and ensuring reproducibility. A closer examination of the frequency distribution plots reveals that the histograms show very reasonable ranges of solutions for  $K$ ,  $h$ ,  $d$ , and  $\alpha$ . This implies that the estimations for these parameters are within the range of their actual values. The frequency distributions of the model parameters for noisy and field examples revealed that the exact points were somewhat moved from the global minimum, depicting some ambiguity in the estimated parameters. These ambiguities though were trivial and still well within permissible limits.

It must be added that in four of the synthetic examples and the Gansu anomaly example, we restricted the search space using historical information. However, one of the objectives of this study was to limit or if possible, eradicate such dependencies. So, for the Bayburt-Sarıhan dyke case, the bounds were left open and the performance of the algorithm assessed.<sup>[2]</sup> From the results, it could be observed that the algorithm still performed excellently even when LB and UB were not explicitly defined presenting a method that can be employed where reconnaissance information is scarce or unavailable.

These features unanimously imply the new methodology is a robust tool, stable and efficient for deciphering the physical characteristics of deep and shallow-seated dykes from magnetic data.

## 5. Conclusion

The use of metaheuristic algorithms to solve complex ill-posed geophysical problems has been around for a while. In fact, these strategies have been found to be more effective than their numerical counterparts in exploring/exploiting potential solution-leading positions.

Nonetheless, despite significant-resolution advancements, several of these strategies employing metaheuristic procedures are still plagued by problems such as premature convergence, local optima, and so on. These discrepancies have necessitated a quest for better-performing inversion methods. The Social Spider Optimization algorithm's capability and effectiveness in modelling the physical parameters ( $K$ ,  $\alpha$ ,  $d$ , and  $h$ ) describing magnetic anomalies from dipping dykes were examined. In contrast to previously studied heuristic algorithms in which a general population concentrating around a single particle vector (best particle) is used to modify individual positions, the SSO algorithm models each individual based on their gender. This strategy encourages the de-individualization of the best-positioned agents, allowing the introduction of computational procedures to mitigate the major problems disturbing traditional techniques. The experiments on both synthetic and real-world anomalies with varying levels of corruption were quite successful. To measure success, model stability was evaluated, and general performance was assessed.

The SSO technique demonstrated both better convergence and solution correctness. Furthermore, uncertainty analysis utilizing the MH sampling algorithm revealed that the geophysical parameters calculated were within high probability ranges. These characteristics point to a competitive processing tool, one that could easily outperform present algorithms. It must be added that while the decoupling of search agents based on gender allowed for more extensive exploration and improved quality resolution, it is observed that this is at the expense of speed.<sup>[1]</sup> This is but a limitation of the algorithm which (as a recommendation) can be improved through modifications and hybridization.<sup>[0]</sup>

As a result, the SSO approach is recommended for inverting geophysical data with higher complexities, such as self-potential and gravity data. It can also be restructured for three-dimensional geophysical problems.